Direct Observation of Standing Wave Formation at Surface Steps Using Scanning Tunneling Spectroscopy

Y. Hasegawa* and Ph. Avouris

IBM Research Division, T. J. Watson Research Center, Yorktown Heights, New York 10598

(Received 10 March 1993; revised manuscript received 1 June 1993)

Using scanning tunneling microscopy and spectroscopy, we have observed the formation of standing waves by the scattering of surface state electrons at steps and defects on the Au(111) surface. From the periods, peak positions, and intensities of the standing waves, the energy dispersion of the surface states, the scattering phase shifts as a function of energy and crystallographic direction, and coherence length could be determined.

PACS numbers: 73.20.At, 61.16.Ch, 72.10.Fk

Crystals imperfections such as point defects, grain boundaries, or surface steps disrupt the periodicity of the crystal potential, and become scattering centers for the electron waves. These scattering phenomena have a profound influence on a number of properties of the solid, including its electrical resistivity, thermoelectric power, magnetic susceptibility, electromigration, and electronic specific heat [1]. The electron-scattering processes are usually studied indirectly through their influence on the above material properties. A macroscopic volume or surface area of the solid is employed and the property is usually studied as a function of the concentration of impurities or imperfections.

In this paper, we present a direct, real-space, nanometer-scale study of electron scattering processes at localized defects using scanning tunneling microscopy (STM) and spectroscopy (STS). Specifically, we discuss the interaction of surface state electrons at the Au(111)-$22\times\sqrt{3}$ surface with steps. At the step, the change in potential leads to the partial reflection of incident electron waves. Interference between the incident and reflected waves results in the formation of standing waves and the modulation of the density of states near the step. We show that this oscillation of the state density can be directly imaged in spatial maps of the differential conductance; such maps can be readily obtained by STS. From these images, important information about the states involved, the scattering process, and subsequent dynamical processes can be easily extracted.

The details of the STM and STS setups used in this study have been described before [2]. All STM experiments were performed in ultrahigh vacuum at room temperature. The Au(111) samples were prepared by evaporation of gold on cleaved mica and subsequent annealing at about 600 °C *in situ* [3] The surface prepared in this way has wide (111) planes [4]. In addition to the simplicity of its preparation, two other factors make it ideal for studies of electron scattering by defects. First, the Au(111) surface has a surface state in the gap of projected bulk states [5,6]. Thus, the electron states are localized near the surface, making them ideally suited for STM probing. Second, the surface state has a simple dispersion: energy minimum at the $\bar{\Gamma}$ point and isotropic dispersion with a positive effective mass. Therefore, the surface state electrons can be treated as a two-dimensional, free-electron-like system.

In Fig. 1(a) we show an STM image of a 320 Å×320 Å area of Au(111) In this image, a step runs from the corner of the upper right to the center of the left side. A small corrugation (~0.1 Å) due to the $22\times\sqrt{3}$ recon-

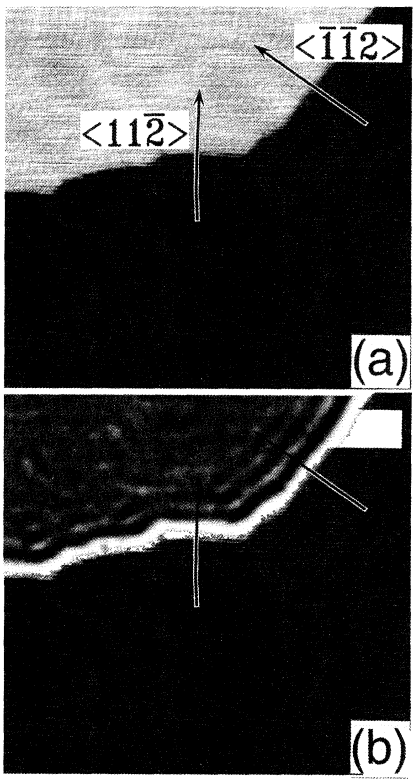

FIG. 1. (a) STM image of a Au(111) surface with a step. The size of the image is about 320 Å×320 Å. (b) Contrast image of the quantity $(dI/dV)/(I/V)$ calculated at +0.15 V from tunneling spectra obtained over the same area shown in the STM image of (a). The stabilizing bias voltage is −1 V.

0031-9007/93/71(7)/1071(4)$06.00

struction, which is characteristic on the Au(111) surface [7-9], is observed. In addition to the topographic image, tunneling spectra have been obtained at 3 Å intervals over the entire area shown in the image of Fig. 1(a). Using the spectroscopic data, a spatial map of the quantity $(dI/dV)/(I/V)$ at a sample voltage of +0.15 V is produced [Fig. 1(b)]. Bright contrast indicates a large value of $(dI/dV)/(I/V)$. It has been shown [10,11] that the value of $(dI/dV)/(I/V)$ provides a rough measure of the local surface density of states (LDOS). Thus, the image of Fig. 1(b) corresponds to a map of the surface LDOS at an energy of 0.15 eV above the Fermi energy level. This image shows a high LDOS right at the step, suggesting the possible formation of a localized step state. In the upper terrace near the step, several bright lines running parallel to the step are seen. As we will discuss later in more detail, the value of $(dI/dV)/(I/V)$ oscillates near steps with a period of about 16 Å in the direction perpendicular to the step. We suggest that this oscillatory structure is due to standing waves formed by the scattering of surface state electrons at steps. Our interpretation is based on studies of the variation of the period and peak positions of these oscillatory structures with the voltage at which the values of $(dI/dV)/(I/V)$ are calculated.

Such data are shown in Fig. 2. This figure was made by laterally averaging the STS data along the $\langle\bar{1}12\rangle$ direction which is normal to the step [see Fig. 1(a)]. [The direction is determined from the pattern of the 22 $\times\sqrt{3}$ reconstruction which is weakly visible in Fig. 1(a).] From these curves we see that the peak positions shift with voltage; they are drawn closer to the step and the period of the oscillation becomes shorter with increasing voltage. Since the voltage at which $(dI/dV)/(I/V)$ is calculated corresponds to the energy of states measured from the Fermi level, our results indicate that LDOS at higher energy has an oscillatory structure near steps with a shorter period.

The change of period with voltage can be related to the energy dispersion of the surface state of Au(111). This dispersion has been determined by photoemission [6] for levels below E_F, and then extrapolated to obtain the behavior of the empty levels (solid line in Fig. 3). The energy of the surface state has a minimum at $k_\parallel=0$ and increases with increasing $k_\parallel$. Our experimental results are consistent with the behavior expected from such a dispersion. The dispersion curve obtained from our experimental results is given in Fig. 3 (open circles). Although the wave numbers at the Fermi level are the same in photoemission and STS, the slopes of the dispersion curves are different. The effective mass calculated by fitting our dispersion data to $E(k)=E_0+\hbar^2k^2/2m^*$ is $m^*=0.15m_e$. This effective mass is significantly smaller than the $m^*=0.28m_e$ obtained by photoemission [6]. It is not clear that the two techniques should give exactly the same dispersion. The STM provides a local measurement near the step. Near steps, the electron density should exhibit an oscillatory behavior, the so-called Friedel oscillation, with a period determined by the Fermi wave number k_F: $\delta n\sim\cos(2k_Fx)$ [12]. As a result, the potential near the steps should also have a component modulated with the same period. The surface state levels can be perturbed by the modulated potential, resulting in a change of their wave number near the steps A numerical solution of the Schrödinger equation in which a potential $U\cos(2k_Fx)$ has been added to the surface potential $U_0(=0.4$ eV) [6] near the step shows that for $U/U_0\simeq0.1$-0.01 the wave number measured by the STM near E_F is given by $k\simeq(k_F+k_\parallel)/2$, where $k_\parallel$ is a wave num-

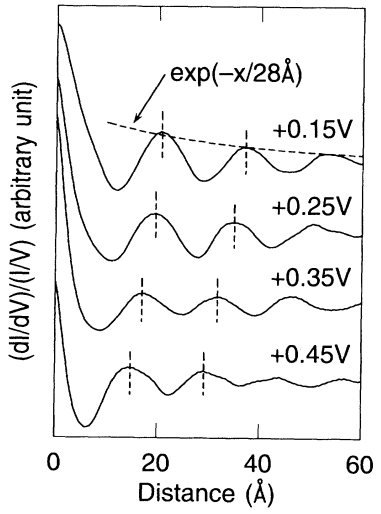

FIG. 2. Plots of $(dI/dV)/(I/V)$ at different sample voltages as a function of the distance from the $\langle\bar{1}12\rangle$ step, showing shifts in peak positions and changes in the period of the oscillatory structure.

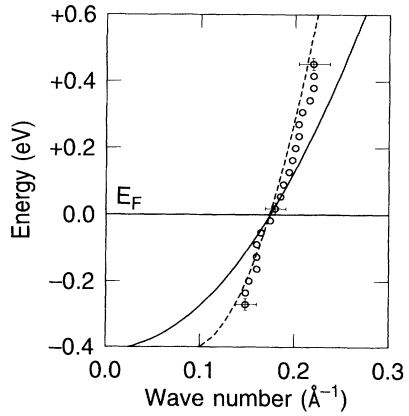

FIG. 3. Energy dispersion of surface states of the Au(111) surface measured by photoemission [6] (solid line) obtained from this experiment (circles), and calculated from $k=(k_F+k_\parallel)/2$ (dashed line), where k_F is the wave number at the Fermi level and $k_\parallel$ is the wave number measured by photoemission.

ber of the Bloch wave state without the modulated potential as is measured by photoemission. As Fig. 3 shows, the agreement of the effective dispersion predicted on the basis of the above considerations (dashed line) and the experimental data is reasonably good. The oscillatory structure is also observed at the lower terrace near the step, although its intensity is weaker than that of the upper terrace suggesting a lower reflection coefficient. Its period, however, is the same as that at the upper terrace, as it should be if our interpretation of the oscillations is correct. We note that an alternative, trivial explanation for the oscillatory structure as a multiple-tip effect can readily be dismissed, given the observed change in the period of the oscillations with bias voltage. Our conclusion is confirmed by two other observations. First, we have observed similar oscillations on two other surfaces: Cu(111) and Ag(111). These systems possess surface states completely analogous to the one on Au(111). The measured wave numbers near E_F agree with the Fermi wave numbers measured by photoemission [6]. Second, in addition to oscillations near steps, we have observed rings around the perimeter of metal islands and rings around individual point defects, indicating scattering and spherical-wave formation by these defects. We also point out that under the conditions of our experiment, the soliton $22\times\sqrt{3}$ surface reconstruction of Au(111) does not interfere with the observation of the surface oscillations. The reconstruction is more prominent in $(dI/dV)/(I/V)$ images of higher voltages [13]. At this point, it should be noted that there have been previous reports of oscillations on graphite surfaces induced by deposited particles or defects [14–16]. However, these oscillations were observed in STM images, not in spectroscopic maps, as in our study, and as a result it was difficult to separate electronic structure from geometric structure and thus quantitatively analyze the oscillations (see discussion below).

Since STM and STS are real-space imaging techniques, important information on scattering which is not easily accessible using diffraction techniques can readily be obtained. One such property is the phase shift of the scattered waves. By measuring the relative position of the step within the period of the oscillatory structure as a function of bias voltage (see Fig. 2), we can obtain the value of the phase shift as a function of the energy of the states. Because the ratio $(dI/dV)/(I/V)$ results in a built-in 180° phase shift upon crossing the zero bias point, the unnormalized differential conductance dI/dV was used for the evaluation of the phase shifts. Figure 4 gives the scattering phase shifts induced by steps perpendicular to the $\langle\bar{1}12\rangle$ and $\langle 11\bar{2}\rangle$ directions. These steps involve (111) and (001) facets, respectively. The shifts induced by both steps are negative, indicating a net repulsive interaction of the electrons with the step. The $\langle\bar{1}12\rangle$ step induces a $-\pi$ phase shift which implies that it acts as a repulsive barrier with a reflection coefficient of unity, $R=1$. At the $\langle 11\bar{2}\rangle$ step the phase shift is about $-\pi/2$. This indicates that there is some transmission of the surface state electrons through this step. By using a simple model of a delta-function potential barrier, a transmission coefficient $T=1-R$ of about 0.1 is obtained. The finite transmission through the $\langle 11\bar{2}\rangle$ step is most likely the result of the more open structure of the (001) facet. The ability to determine reflection coefficients for electrons near E_F from a particular atomic scale structure implies that one can determine the contribution of such an individual structure to the electrical resistance [17].

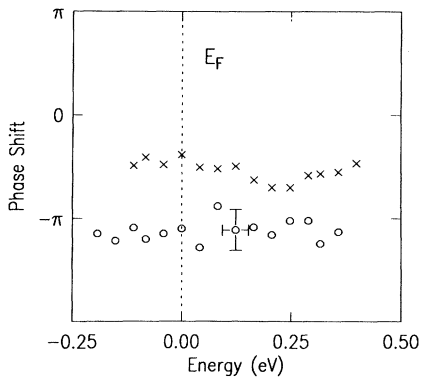

FIG. 4. A plot of the scattering phase shifts as a function of the energy of the states involved, measured at the $\langle\bar{1}12\rangle$ step (circles) and at the $\langle 11\bar{2}\rangle$ step (crosses).

In the absence of additional scattering mechanisms the oscillations, produced by a potential $U(R)$, should decay as $\sim R^{-(\nu+3)/2}$, where ν is the dimensionality of R [18]. At $T\neq 0$ in a real solid the coherence of electronic states can be broken by additional scattering processes involving phonons, impurities, and defects. These processes lead to an effective electron mean free path or coherence length l_c, and the oscillations are expected to decay as $\exp(-R/l_c)$ [18]. The decay of the STM-detected oscillations is better fitted by an exponential rather than a power law. The coherence lengths determined in the energy range studied are in the 30–40 Å range. The possibility that the coherence is limited by scattering by point defects [19] can be excluded. In our spectroscopic maps, we do observe scattering by point defects. The scattering appears as a set of concentric rings surrounding the defect. The density of such defects, however, is not capable of accounting for the observed l_c. Without measurements at different temperatures, the possible role of phonons in dephasing cannot be ascertained. However, another effect of temperature, that is, the thermal width of the STM beam appears capable of explaining our results. From the Fermi distribution, one obtains a width ΔE (FWHM) of $\sim 3.5k_BT$, which is substantial ($\sim$0.09 eV) at room temperature. This thermal width can be related, through the dispersion relation of the surface state, to a wave-number spread of $\Delta k_{\parallel}=(m^*\Delta E)/(\hbar^2 k_{\parallel})$. The coherence length l_c will then be $l_c\sim 1/\Delta k_{\parallel}$. At room temperature, a coherence length of $\sim$50 Å is predicted, in rough agreement with our observations. It thus appears

that dephasing due to the $\Delta k_{\parallel}$ spread of the electron wave packet can be responsible for the observed decay. If this is true, then substantial enhancement of the oscillations will be achieved by operating at low temperatures.

In conclusion, using STS, we have observed the standing waves produced by the scattering of surface state electrons at steps of the Au(111) surface. The dispersion of the states, the energy and crystallographic direction dependence of the scattering phase shifts, and the coherence length of the surface state electrons can be directly obtained from the spectroscopic maps. This study shows that STS maps can provide a powerful new approach for the real-space observation and study of electron scattering by individual point and extended defects.

We acknowledge valuable discussions with I.-W. Lyo, R. E. Walkup, C. Lutz, and D. M. Newns.

Note added.—After the submission of our manuscript we became aware of similar work on Cu(111) by M. F. Crommie, C. P. Lutz, and D. M. Eigler, Nature (London) **363**, 524 (1993).

*Present address: Mesoscopic Materials Research Center, Kyoto University, Kyoto, 606-01 Japan.

[1] N. W. Ashcroft and N. D. Mermin, *Solid State Physics* (Saunders College, Philadelphia, 1976).
[2] R. Wolkow and Ph. Avouris, Phys. Rev. Lett. **60**, 1049 (1988).
[3] Y. Hasegawa and Ph. Avouris, Science **253**, 1763 (1992).
[4] V. M. Hallmark *et al.*, Phys. Rev. Lett. **59**, 2879 (1987).
[5] D. Woodruff, W. A. Royer, and N. V. Smith, Phys. Rev. B **34**, 764 (1986).
[6] S. D. Kevan and R. H. Gaylord, Phys. Rev. B **36**, 5809 (1987).
[7] Ch. Wöll *et al.*, Phys. Rev. B **39**, 7988 (1989).
[8] J. V. Barth *et al.*, Phys. Rev. B **42**, 9307 (1990).
[9] D. D. Chambliss, R. J. Wilson, and S. Chiang, Phys. Rev. Lett. **66**, 1721 (1991).
[10] R. M. Feenstra, J. A. Stroscio, and A. P. Fein, Surf. Sci. **181**, 295 (1987).
[11] N. Lang, Phys. Rev. B **34**, 5947 (1986).
[12] J. Freidel, Nuovo Cimento Suppl. **2**, 287 (1958).
[13] M. P. Everson and R. C. Jacklevic, J. Vac. Sci. Technol. A **8**, 3662 (1990).
[14] T. R. Albrecht *et al.*, Appl. Phys. Lett. **52**, 362 (1988).
[15] H. A. Mizes and J. S. Foster, Science **244**, 559 (1989).
[16] J. Xhie *et al.*, Phys. Rev. B **43**, 8917 (1991).
[17] R. Landauer, Z. Phys. B **68**, 217 (1978).
[18] I. Adawi, Phys. Rev. **146**, 379 (1966).
[19] J. Tersoff and S. D. Kevan, Phys. Rev. B **28**, 4267 (1983).

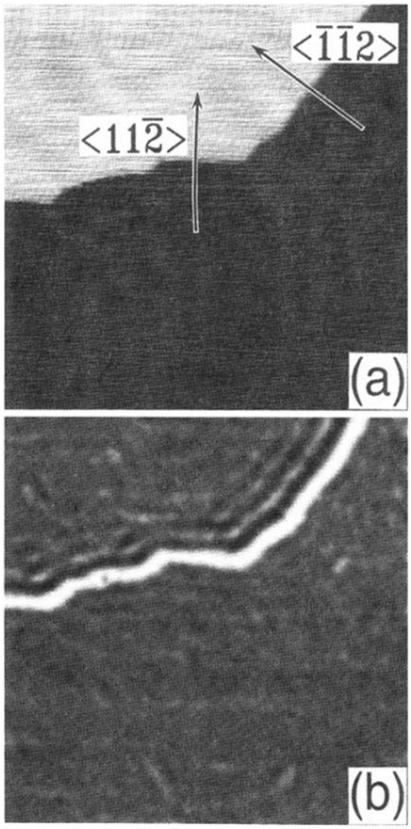

FIG. 1. (a) STM image of a Au(111) surface with a step. The size of the image is about 320 Å×320 Å. (b) Contrast image of the quantity $(dI/dV)/(I/V)$ calculated at +0.15 V from tunneling spectra obtained over the same area shown in the STM image of (a). The stabilizing bias voltage is −1 V.